

Molecular dynamics simulation of the effect of adding an Al₂O₃ nanoparticle to PEO–LiCl/LiBr/LiI systems

Heiki Kasemägi,^{a,d} Mattias Klintonberg,^{b,c} Alvo Aabloo^a and John O. Thomas*^d

^aTechnology Centre, Tartu University, Tähe 4, 51010 Tartu, Estonia

^bCondensed Matter Theory Group, Department of Physics, Uppsala University, Box 530, SE-751 21 Uppsala, Sweden

^cLawrence Berkeley National Laboratory, University of California, Berkeley, USA

^dMaterials Chemistry, Ångström Laboratory, Uppsala University, Box 538, SE-751 21 Uppsala, Sweden. E-mail: josh.thomas@mkem.uu.se

Received 14th August 2001, Accepted 4th September 2001

First published as an Advance Article on the web 7th November 2001

The effect of adding *ca.* 20 Å diameter quasi-spherical nanoparticles of α -Al₂O₃ (corundum) to LiCl, LiBr and LiI salts in amorphous PEO has been simulated at a nominal 360 K by molecular dynamics (MD) methods; the Li:EO ratio studied was 1:10, along with salt-free and particle-free reference cases. The PEO forms an immobilised coordination sphere around the particle. Li-ion mobility in PEO is found to decrease on the addition of particles; the effect is greatest near the particle surface in the region of the PEO. LiX pairing/clustering (for X=Cl, Br, I) was observed away from the particle surface; the effect was greatest for LiBr and least for LiCl. The ion-clustering tendency would appear to be dependent on the particle size; it is noticeably larger for the case of smaller particles. A number of unpaired Li ions were found attached to the particle within the region of the immobilised PEO. Corresponding “free” anions were located somewhat further away from the particle surface in the more mobile PEO regions, along with charged and uncharged ion-clusters.

Introduction

Poly(ethylene oxide) (PEO)-based polymer electrolytes have been the object of considerable interest for several decades, mainly through their potential use as polymer electrolytes in electrochemical devices. However, at ambient temperatures, PEO-based electrolytes are generally poor ion conductors ($\sigma < 10^{-8}$ S cm⁻¹) due to their high degree of local crystallinity.¹ A number of salts, *e.g.* RbSCN, RbI, CsSCN, CsI and Hg(ClO₄)₂, actually form low-temperature amorphous phases with PEO at relatively high salt concentrations but, with the major interest centred on lithium-based electrochemical devices, amorphous lithium-salt/polymer electrolytes are desirable. Reasonable conductivity in lithium-salt/PEO electrolytes can be achieved (*ca.* 10⁻⁵ S cm⁻¹) around 100 °C, but the mechanical properties of these polymer materials are poor.

There has therefore been a strong focus in recent years on obtaining improved ambient temperature Li-ion conductivity, improved mechanical stability, and electrochemical stability with respect to active electrode materials. Most recently, attention has turned to the incorporation of nanosize particles into ionically conducting polymers in order to improve their ion conductivities. For example, Krawiec *et al.*² found that adding nanosize particles of α -Al₂O₃ to (PEO)₈-LiBF₄ increased its conductivity by an order of magnitude compared to that obtained using micron-size particles. This conductivity enhancement has been found to be dependent on filler concentration; maximum ionic conductivity was obtained for 10 wt.% nanosize Al₂O₃. Croce *et al.*³ could demonstrate conductivity enhancement in PEO–LiClO₄ mixtures containing both TiO₂ and Al₂O₃ nanoparticles (diameter 6–130 Å) in the temperature range of 30–80 °C. It was later shown by Capiglia *et al.*⁴ that the addition of nanoscale SiO₂ filler-particles to the (PEO)₈-LiClO₄ and (PEO)₈-LiN(CF₃SO₂)₂ systems increases the conductivity by more than an order of magnitude; the effect was again shown to be filler-concentration dependent. It was

also claimed by Sun *et al.*⁵ that the addition of micron-size particles of the ferroelectric BaTiO₃ (diameter: 0.6–1.2 µm) to PEO–LiClO₄ enhanced its ionic conductivity

The effect of salt concentration under constant filler-concentration condition has been studied by Best *et al.*⁶ An amorphous polyether triol with ethylene and propylene oxide units in 3:1 ratio (3PEG) was studied for LiClO₄ and LiN(CF₃SO₂)₂ (LiTFSI) in different concentrations, and 10 wt.% TiO₂ filler. The filler appears to increase the conductivity at higher salt concentrations. This was suggested to occur for the case of LiClO₄ by lowering the degree of ion aggregation within the polymer–salt mixture as a result of competing interactions between salt-ions and filler. This was explained in the case of LiTFSI by a lower degree of ion aggregation. On the other hand, Wieczorek *et al.*⁷ have shown that the conductivity increases with salt concentration in the low molecular weight poly(ethylene glycol) (PEG)–LiClO₄ system with α -Al₂O₃ nanoparticles as filler. The conductivity was shown by Strauss *et al.*⁸ to reach a maximum at $n=20$ in the LiI–(PEO)_{*n*}-Al₂O₃ system. Also, more ion-pairs were found in the composite polymer electrolyte case; these pairs reduce the effective concentration of charge carriers and contribute an additional term in the diffusion impedance.

A number of molecular dynamics (MD) simulations have been made by our group of the properties of crystalline⁹ and amorphous¹⁰ PEO containing various lithium-salt ions; and of surface properties of related PEO–salt systems.^{11–13} The aim of this paper is to provide some deeper insights into the behaviour of nano-composite polymer electrolytes. This we achieve by simulating a series of models involving amorphous PEO containing Li salts and nanosize Al₂O₃ (corundum) particles. Models involving amorphous PEO alone, and PEO with salt or filler alone are studied as reference states. MD simulations were made for LiCl, LiBr and LiI as dopant salts for an Li:EO ratio of 1:10.

The models

Neutral pieces of α -Al₂O₃ (corundum) were extracted from its rhombohedral crystal structure (space group: $R\bar{3}c$ (no. 167);¹⁴ unit-cell parameters: $a=4.75$ Å, $c=12.99$ Å (hexagonal setting)).¹⁵ These particles were then “computer-annealed” at 2000 K to give them roughly spherical forms (diameters: 14 Å and 18 Å; 115 and 335 atoms, respectively) and with oxygen atoms at their surfaces. The simulation boxes were then filled with PEO by controlled pivotal Monte Carlo growth around the particles.

A total of 12 models were simulated: two particle-sizes (14 Å and 18 Å); three salts (LiCl, LiBr and LiI); and six reference states (PEO alone, PEO with two particle-sizes and no salt, PEO with three salts and no particle). The simulation boxes were as follows:

(1) A rectangular particle-free and salt-free reference box ($26 \times 21 \times 22$ Å) containing an amorphous PEO chain of 200 EO monomers.

(2) Cubic reference simulation boxes containing particles:
(1) box size $31 \times 31 \times 31$ Å; ~ 14 Å diameter particle; 455 EO monomers;
(2) box size $37 \times 37 \times 37$ Å; ~ 18 Å diameter particle; 787 EO monomers.

(3) A rectangular particle-free reference box ($26 \times 21 \times 22$ Å) containing an amorphous PEO chain of 200 EO monomers and three different lithium-salts.

(4) Cubic simulation boxes containing PEO, salt and particle:
(1) box size $31 \times 31 \times 31$ Å; 14 Å diameter particle; 455 EO monomers; *ca.* 6% of the total volume, and 10% of the total mass were occupied by the particle; the particle surface-area was $300 \text{ m}^2 \text{ cm}^{-3}$.
(2) box size $37 \times 37 \times 37$ Å; 18 Å diameter particle; 787 EO monomers; particle filling was here *ca.* 10% of the total volume and 16% of the total mass; the particle surface-area was $600 \text{ m}^2 \text{ cm}^{-3}$.

The simulation box sizes were chosen to leave the minimum distance between the particle surfaces in the periodic arrangement of particles the same as the particle diameters in the two cases. Unpaired lithium-salt ions were inserted randomly into the PEO host with an Li:EO ratio of 1:10.

The molecular dynamics (MD) simulation method

MD simulation involves the simultaneous solution of Newton's equations of motion for all atoms (or ions) in an appropriately chosen simulation box. A local version of DL_POLY¹⁶ with force fields developed earlier for PEO,⁹ β "-alumina,¹⁷ LiBr and Br-PEO,^{18,19} LiCl, LiI, Li-PEO, Cl-PEO and I-PEO.²⁰ The long-range interaction potentials were described by eqn. (1):

$$U(r) = A \exp\left(-\frac{B}{r}\right) - \frac{C}{r^6} - \frac{D}{r^4} + \frac{q_1 q_2}{4\pi\epsilon_0 r} \quad (1)$$

The parameters used are listed in Table 1.

The MD simulations used periodic boundary conditions and an Ewald summation to calculate the electrostatic forces at longer distances. Each simulation consisted of an equilibration period of 50 ps followed by *NVT* simulation (number of particles (N), volume (V) and temperature (T) constant) for 100 ps, followed by *NpT* simulation (Nose–Hoover model: N , pressure (p) and T constant) for up to 800 ps at nominal temperature 360 K. Sampling was made every 1 ps (every 1000 time-steps) in the simulation. Models were prepared on a local array of PCs, and the MD simulations carried out on an IBM Power Parallel SP supercomputer at the Parallel Computer Centre (PDC) of the Royal Institute of Technology (KTH) in Stockholm; a total of 36000 CPU hours was used.

Table 1 Potential parameters describing the long-range interactions (O_{et}: ether oxygen; O_{Al}: particle oxygen)

Atom pair	$A/\text{kcal mol}^{-1}$	$B/\text{\AA}$	$C/\text{kcal \AA}^6 \text{mol}^{-1}$	$D/\text{kcal \AA}^4 \text{mol}^{-1}$
O _{et} ...O _{et}	58298.9	0.24849	192.1	0.0
O _{et} ...C	42931.6	0.27550	352.8	0.0
O _{et} ...H	20432.6	0.24450	98.8	0.0
O _{et} ...Al	928077.6	0.24997	1139.9	0.0
O _{et} ...O _{Al}	951969.6	0.15784	239.7	0.0
C...C	31615.1	0.30251	647.8	0.0
C...H	15046.7	0.27151	181.5	0.0
C...Al	170201.1	0.30315	2160.9	0.0
C...O _{Al}	1172167.0	0.24855	4537.0	0.0
H...H	7161.2	0.24050	50.8	0.0
H...Al	110177.8	0.26812	669.5	0.0
H...O _{Al}	998796.7	0.19945	919.0	0.0
Al...Al	0.0	0.10000	0.0	0.0
Al...O _{Al}	33652.8	0.29912	0.0	0.0
O _{Al} ...O _{Al}	524957.1	0.14900	530.4	0.0
Li...O _{et}	191106.0	0.17510	0.0	76.9
Li...C	8140.0	0.37994	0.0	76.9
Li...H	13139.0	0.22852	0.0	77.4
Li...Al	53082940.0	0.14873	0.0	0.0
Li...O _{Al}	62774060.0	0.11668	0.0	0.0
Li...Li	44195.0	0.13742	0.0	9.3
Li...Br	30563.7	0.39879	0.0	2916.7
Li...Cl	30868.0	0.31797	0.0	729.4
Li...I	23625.0	0.41034	0.0	2108.7
Br...O _{et}	50059.4	0.30488	313.1	621.4
Br...C	18714.6	0.39014	3099.2	20.7
Br...H	8234.8	0.34214	391.8	0.0
Br...O _{Al}	40369390.0	0.15673	2263.9	0.0
Br...Al	2958746.0	0.27148	13428.4	0.0
Br...Br	195631400.0	0.19305	0.0	2149.8
Cl...O _{et}	40353.0	0.31056	1005.0	536.3
Cl...C	17926.0	0.36590	1273.3	67.2
Cl...H	7543.0	0.32701	263.0	0.0
Cl...O _{Al}	654978.0	0.23133	491.7	0.0
Cl...Al	2633313.0	0.27671	14322.4	0.0
Cl...Cl	70768.4	0.39622	29699.1	0.0
I...O _{et}	52238.0	0.33910	2604.0	712.4
I...C	23213.0	0.40617	3301.0	77.7
I...H	9764.0	0.35881	682.5	0.0
I...O _{Al}	40369390.0	0.14686	3619.7	0.0
I...Al	3236445.0	0.28076	19481.8	0.0
I...I	1898731000.0	0.17742	0.0	2734.4

Results and discussion

Structural effects

The ultimate purpose of this work is to study the influence of nanosize inorganic particles on the salt-in-PEO system (Fig. 1). Let us first consider, however, the changes in the particle and PEO *structure* after adding the nanoparticle and the salt to PEO (particles of 14 Å diameter and 18 Å diameter will be referred to hereafter as 14 Å and 18 Å particles).

We see from Fig. 2 that the surface of the generated 18 Å particle is well defined, with O_{Al} atoms tending to lie outermost with five-fold Al–O_{Al} coordination. In corundum, the Al–O_{Al} coordination is six-fold, but we see that the radial distribution function for the particle (Fig. 3) shows average coordination number to be five. This is because the simulated particle is of nanosize and is thus essentially “all-surface and no-bulk”. This distribution is found to remain virtually unchanged for both the particle-in-PEO and particle-in-salt-in-PEO systems.

Let us consider now what happens to the PEO host structure on adding the nanosize particle. There is clearly a region of high ether-oxygen (O_{et}) concentration *ca.* 3 Å outside the particle surface for both particle radii (Fig. 4). The polymer chain tends to curl itself around the particle to form a “coordination sphere” (Fig. 5(a)). Note that this effect is not a result of the polymer simply being forced away from the inserted particle; on the contrary, the polymer was generated so

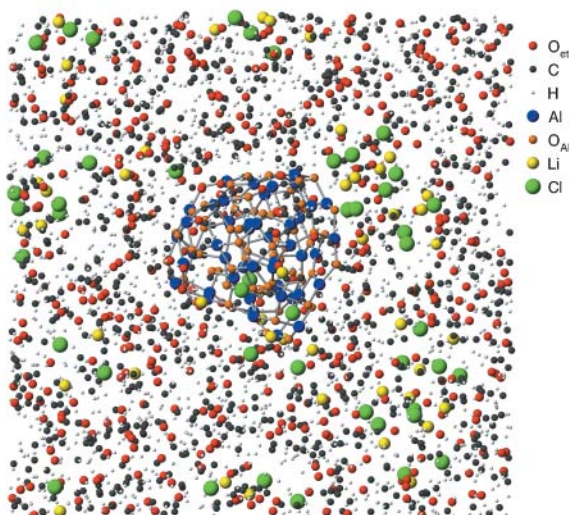


Fig. 1 Simulation box for the case of a 14 Å diameter Al_2O_3 particle in amorphous $\text{LiCl}(\text{PEO})_{10}$.

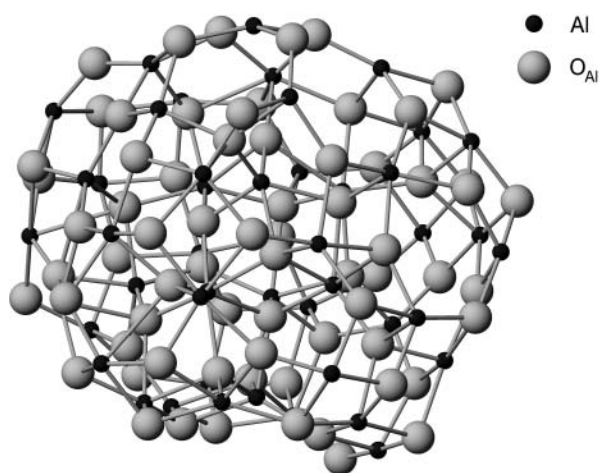


Fig. 2 Atomic-level structure of the 14 Å diameter Al_2O_3 particle after simulated annealing.

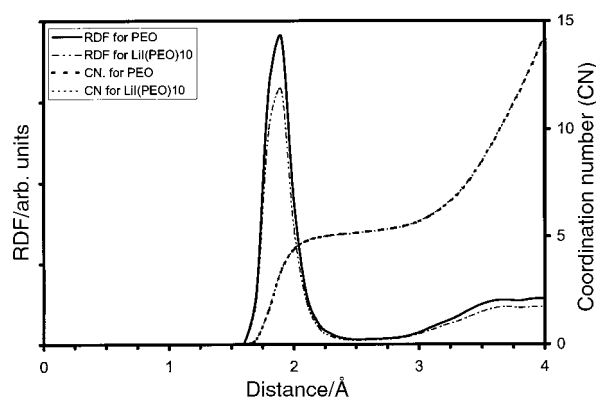


Fig. 3 Radial distribution function for $\text{Al}\cdots\text{O}_{\text{Al}}$ for the case of the 18 Å particle in PEO and $\text{LiI}(\text{PEO})_{10}$ (O_{Al} -particle oxygen).

as to fill the space left in the simulation box around the particle. Note also that it is not a continuous section on PEO that curls itself around the particle, but rather that the same chain approaches and leaves the particle at several points along its length, with up to five successive O_{et} atoms in close proximity to the particle.

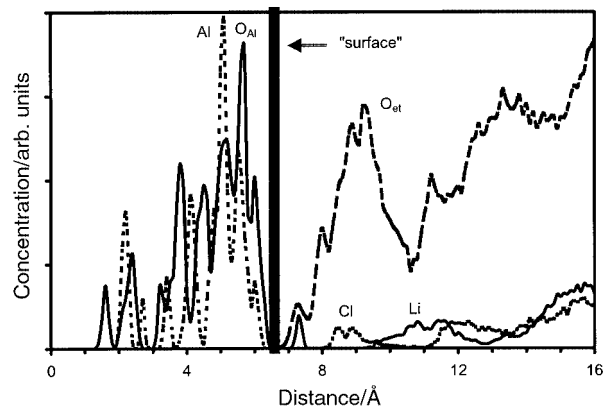


Fig. 4 Atom density distribution for the 14 Å diameter Al_2O_3 particle in $\text{LiCl}(\text{PEO})_{10}$.

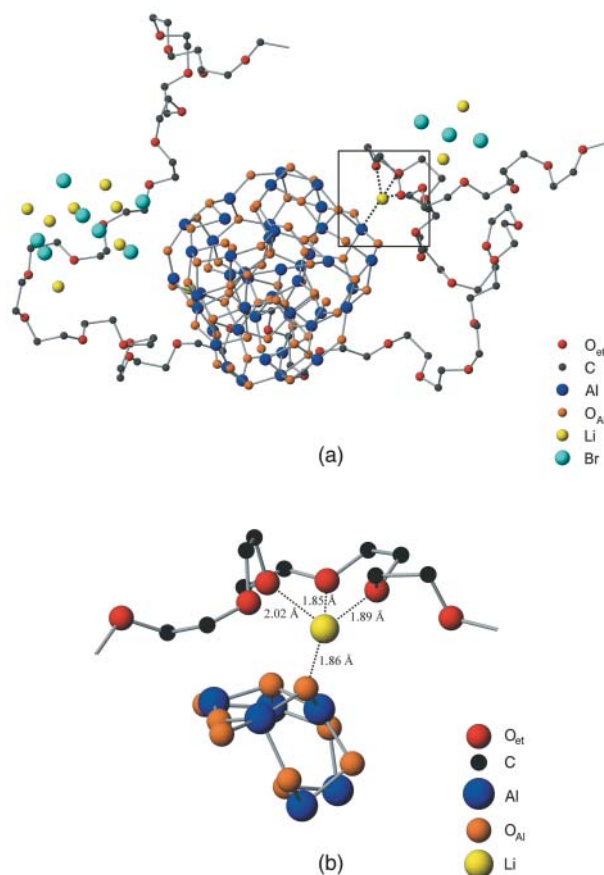


Fig. 5 (a) PEO chain around the 14 Å particle with Li- and Br-ions; (b) an example of the detailed structure around a Li^+ ion bound to the particle.

So now to the effect of adding salt to PEO: we have studied three monoatomic anion cases: $\text{LiX}(\text{PEO})_{10}$ for $\text{X} = \text{Cl}, \text{Br}$ and I ; in practice, more complex polyatomic anions like BF_4^- , PF_6^- , “triflate” $[\text{CF}_3\text{SO}_3^-]$ and “TFSI” $[\text{N}(\text{CF}_3\text{SO}_2)_2^-]$ are more commonly exploited in a battery context, due largely to their less concentrated distribution of negative charge. Li-X radial distribution functions (RDFs) are seen to have sharp first peaks at 2.25, 2.50 and 2.70 Å for LiCl , LiBr and LiI , respectively (see Fig. 6 for LiI results). The coordination numbers (CN) show clear plateaus corresponding to these peaks at 1.5 for LiCl , 2.4 for LiI (Fig. 6), and 2.7 for LiBr . This suggests a tendency to form ion-clusters for LiI and LiBr and ion-pairs and -clusters for LiCl . Similar clustering tendencies have been seen in simulations of LiI in $(\text{PEO})_x\text{LiI}$ ($x = 100, 50, 25, 16$ and

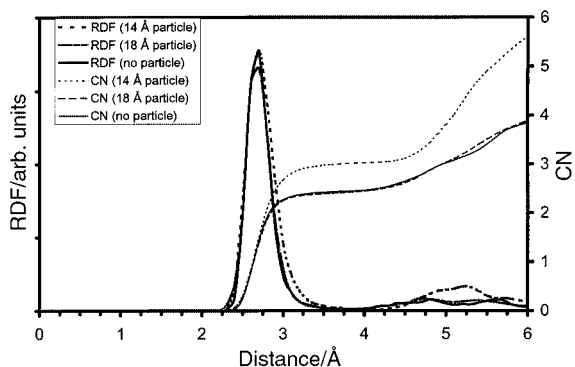


Fig. 6 Radial distribution function for Li...I for the case of LiI(PEO)₁₀ and 14 Å and 18 Å particles in LiI(PEO)₁₀.

8) by Müller-Plathe and van Gunsteren,²¹ ion-pairing has also been observed for LiClO₄ in MD simulations of amorphous PEO by Halley *et al.*²²

The most interesting phenomena to probe are, of course, those resulting from adding the particle to the salt-in-PEO system. Some dissociated lithium ions are found to collect between the particle surface and the surrounding PEO. An example of the local environment of one such lithium ion is shown in Fig. 5(b); it coordinates to three O_{et} atoms and to one particle-oxygen O_{AI} which is, in turn, itself two-fold coordinated to Al-atoms.

The ion-pairing and -clustering effects discussed above for the salt-in-PEO system increase on adding the particle; the coordination number for LiI is higher after adding the 14 Å particle to the salt-in-PEO system (Fig. 6); rising from 2.45 to 3.0. While a few lithium ions are found near the particle surface, the remaining lithiums and most of the anions participate in cluster- and pair-formation away from the particle (Fig. 4). Only very few anions can be considered as “free” and not belonging to any ion-cluster or ion-pair. Cluster sizes vary greatly, involving from 3 to as many as 30 ions for the 14 Å particle case (Fig. 7). The clusters are either neutral or carry +1 to -2 charges. One of the main effects of adding the

particle is thus to increase ion-association. The clusters tend to contain more ions on the addition of a particle than in the salt-in-PEO cases alone, and these clusters are located away from the particle.

Dynamical effects

The dynamical effects of adding a nanoparticle to the salt-in-PEO system can also be extracted from the MD simulations. We see, not surprisingly, that the Al and O_{AI} atoms vibrate somewhat more at the particle surface than near its centre (Fig. 8), and that this effect is virtually unchanged between the particle-in-PEO and particle-in-salt-in-PEO cases. The effect of both polymer and salt on atomic-level motion in the particle is clearly negligible.

The same cannot be said of the effect of the particle on PEO dynamics; the PEO chain is clearly immobilised in its “coordination sphere” around the particle (Fig. 9), considerably more mobile away from the particle; but still less mobile than in particle-free PEO. Interestingly, the ether-oxygens are seen to be more mobile both near and “away from” the 18 Å particle than the 14 Å particle. This could well be an unfortunate

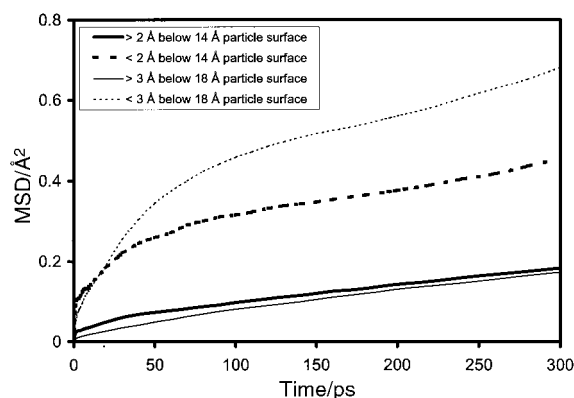


Fig. 8 Mean-square-displacement (MSD) for Al for the cases of 14 Å and 18 Å particles in PEO.

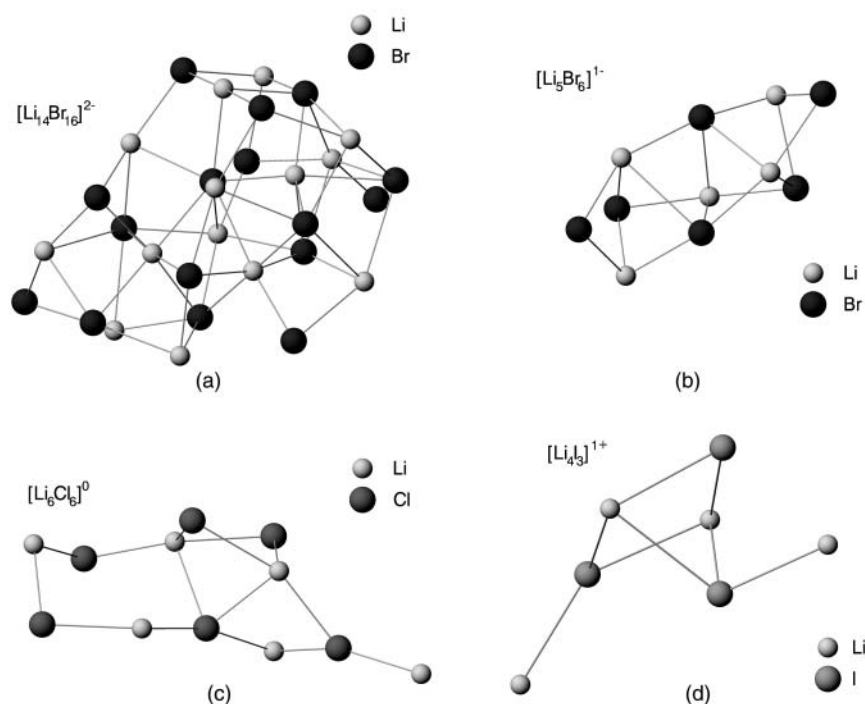


Fig. 7 Examples of ion-clustering: (a) [Li₄Br₁₆]²⁻ for a 14 Å particle; (b) [Li₅Br₆]¹⁻ for a 14 Å particle; (c) [Li₆Cl₆]⁰ for a 14 Å particle; (d) [Li₄I₃]¹⁺ for an 18 Å particle.

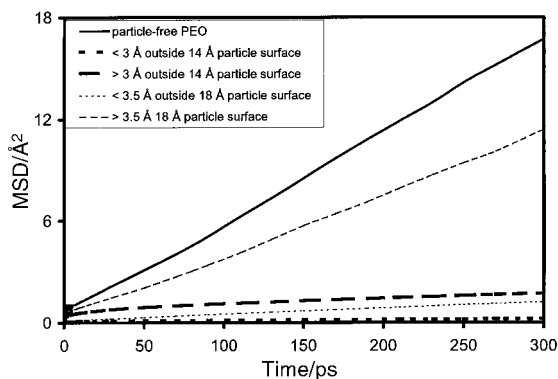


Fig. 9 Mean-square-displacements for ether O atoms in the case of 14 Å and 18 Å diameter Al_2O_3 particles in PEO.

artefact of the arbitrary condition that the distance between the particles is equal to the particle diameter, since we must have more “bulk” PEO in the 18 Å particle case. The “coordination sphere” remains rigid and immobilised in all simulated systems. This “rigid coordination sphere” formed around the particle appears to expel most of the ions to regions away from the particle surface, thus causing the relative increase in ionic concentration away from the particle surface and consequent higher ion-clustering effects; a small number of lithium ions remain bonded to the particle.

We also see that lithium ions show higher mobility in the salt-in-PEO than in the particle-in-salt-in-PEO cases, with a minimal Li-ion mobility near the particle surface, and higher Li-ion mobility away from the particle surface; but still not approaching the Li-ion mobility in the particle-free cases (Fig. 10). Also, Li-ion mobility in the PEO tends to be higher away from the larger particle. Moreover, the mobilities for Cl^- , Br^- and I^- anions tend to be comparable to and, in some cases, even higher than those of the lithium ions.

Conclusions

The results presented here are an excellent illustration of what can realistically be achieved through MD simulation of a system of this relative complexity, although they perhaps do not give any absolutely definitive answers. A number of clear qualitative observations can be made:

(1) The most reliable indications to emerge are of the immobilisation of a small number of Li^+ ions (*ca.* 3–5) near the surface of the nanoparticle. We also see that the clusters formed (although they can be large) will tend to be either neutral or carry a small excess charge (+2 to –1) (see the histogram in Fig. 11). The simulations made here give no indication as to the dissociation properties of these clusters as they approach the

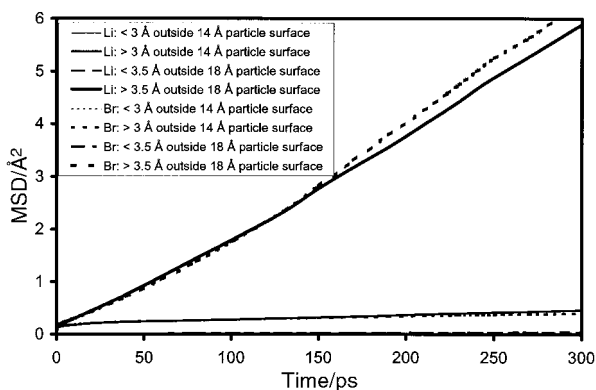


Fig. 10 Mean-square-displacement for Li^+ and Br^- ions for the cases of 14 Å and 18 Å particles in $\text{LiBr}(\text{PEO})_{10}$.

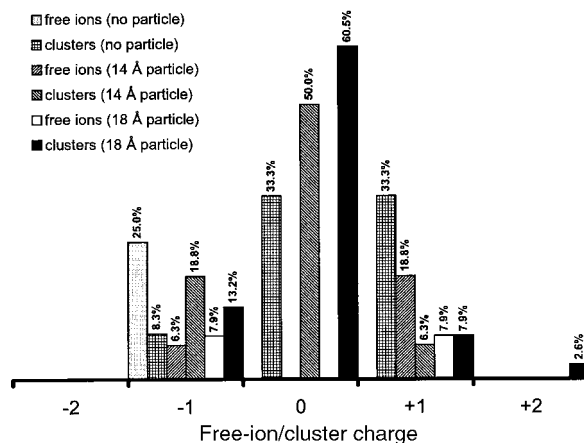


Fig. 11 A histogram showing the distribution of free-ion/cluster charges for the LiCl systems.

electrolyte–electrode interface. It is actually this which controls the battery-related properties of a given polymer–salt–electrode combination.

(2) This Li^+ immobilisation has a significant secondary effect; namely, that these bound lithiums also attract and coordinate the O_{et} atoms of the PEO chain, resulting in regions of immobilised PEO in a “coordination shell” around the nanoparticle. Although successive O_{et} atoms along the PEO chain do not wrap themselves around the nanoparticle (the chain tends to make and break contact with the particle at several points along its length), the analogy with a “first hydration sphere” around a positive ion in a water–salt solution is clear. Outside this “first shell”, the PEO and salt ions are significantly more mobile.

(3) It is in these outer regions that the ion-pairing and ion-clustering phenomena appear, and it is apparent that these effects are significantly greater for the smaller diameter particle. More careful attention must be paid here to the choice of model parameters; it is also more relevant from a battery point of view to study polyatomic anions (triflate, imide, PF_6^- , BF_4^- , *etc.*), in which the negative charges are more spatially dispersed over their surfaces, thereby rendering them less prone to ion-aggregation effects.

(4) One of the few pieces of solid experimental evidence of the effect of particle addition is the disappearance of the so-called DLAM-mode related to the damping of librational motion of the PEO, as the PEO becomes bound to the particle.⁶ This is, indeed, well predicted by the simulation—where several sections along the PEO length (up to 5 O_{et} atoms) are seen to become bound to the particle and essentially rigid. The naïve picture that this effect would expel excess positive charge into the PEO bulk would not appear to apply, however. It would rather appear that the immobilised PEO helps to bind positively charged Li ions near to the particle surface—thus expelling negative charge carriers into the PEO bulk. These simplistic pictures must be further probed in future studies, however.

In retrospect, we see then that there are many *model parameters* that could perhaps have been chosen in a more optimal manner to fully realise our original goal of actually probing the effect of adding a nanoparticle to a PEO–salt system, *e.g.*:

(1) the *salt concentration* could have been lower to avoid the serious ion-pairing and ion-clustering effects described above.

(2) the effective *simulation temperature* must also be carefully tuned: if set too high, we risk large ion-aggregation effects (as seen here); set too low, and the simulations take an unrealistically long calculation time. We see now that we may have chosen somewhat too high a simulation temperature (360 K); 300–320 K would perhaps have been optimal.

(3) parameters relating to *model geometry* (particularly particle and simulation-box dimensions) can also have had a decisive effect on the results which have emerged. We have here ensured that the minimum distance between the particles is the *same* as the chosen particle diameter. Other choices could have been made, and might well have led to qualitatively different results.

Acknowledgements

This work has been supported by grants from the Swedish Natural Science Research Council (NFR). Stipendia to Heiki Kasemägi from the Nordic Energy Research Programme (NEFP), the Kami Research Foundation (KFS) and the Estonian Science Foundation (ETF) are all gratefully acknowledged, as is the fine service provided by the Stockholm Parallel Computer Centre (PDC). We also wish to thank Dr Patrik Johansson of CTH, Gothenburg for his force field parameters for LiBr.

References

- 1 F. M. Gray, *Polymer Electrolytes*, The Royal Society of Chemistry, Cambridge, 1997.
- 2 W. Krawiec, L. G. Scanlon, Jr., J. P. Fellner, R. A. Vaia, S. Vasudevan and E. P. Giannelis, *J. Power Sources*, 1995, **54**, 310.
- 3 F. Croce, G. B. Appetecchi, L. Persi and B. Scrosati, *Nature*, 1998, **394**, 456.
- 4 C. Capiglia, P. Mustarelli, E. Quartarone, C. Tomasi and A. Magistris, *Solid State Ionics*, 1999, **118**, 73.
- 5 H. Y. Sun, H.-J. Sohn, O. Yamamoto, Y. Takeda and N. Imanishi, *J. Electrochem. Soc.*, 1999, **146**, 1672.
- 6 A. S. Best, A. Ferry, D. R. MacFarlane and M. Forsyth, *Solid State Ionics*, 1999, **126**, 269.
- 7 W. Wieczorek, P. Lipka, G. Zukowska and H. Wycilik, *J. Phys. Chem. B*, 1998, **102**, 6968.
- 8 E. Strauss, D. Golodnitsky, G. Ardel and E. Peled, *Electrochimica Acta*, 1998, **43**, 1315.
- 9 S. Neyertz, D. Brown and J. O. Thomas, *J. Chem. Phys.*, 1994, **101**, 10064.
- 10 S. Neyertz, D. Brown and J. O. Thomas, *Comput. Polym. Sci.*, 1995, **5**, 107.
- 11 A. Aabloo and J. O. Thomas, *Comput. Theor. Polym. Sci.*, 1997, **7**, 47.
- 12 A. Aabloo and J. O. Thomas, *Electrochim. Acta*, 1998, **43**, 1361.
- 13 A. Aabloo, M. Klintonberg and J. O. Thomas, *Electrochim. Acta*, 2000, **45**, 1425.
- 14 *International Tables for Crystallography, Vol. A: Space-Group Symmetry*, ed. T. Hahn, 4th revised edn., 1996.
- 15 T. C. Huang, W. Parrish, N. Masciocchi and P. W. Wang, *Adv. X-Ray Anal.*, 1990, **33**, 295.
- 16 The DL_POLY Project, W. Smith and T. Forester, TCS Division, Daresbury Laboratory, Daresbury, Warrington WA4 4AD, England.
- 17 S. Edvardsson, M. Klintonberg and J. O. Thomas, *Phys. Rev. B*, 1996, **54**, 17476.
- 18 P. Johansson, personal communication.
- 19 A. K. Rappe, C. J. Casewit, K. S. Colwel, W. A. Goddard III and W. M. Skiff, *J. Am. Chem. Soc.*, 1992, **114**, 10024.
- 20 G. D. Smith, R. L. Jaffe and H. Partridge, *J. Phys. Chem. A*, 1997, **101**, 1705.
- 21 F. Müller-Plathe and W. F. van Gunsteren, *J. Chem. Phys.*, 1995, **103**, 4745.
- 22 J. W. Halley, Y. Duan, L. A. Curtiss and A. G. Baboul, *J. Chem. Phys.*, 1999, **111**, 3302.